Dielectronic recombination versus charge exchange: Electron capture by metastable ions

S. Bliman
CNRS URA 775, Laboratoire de Spectroscopie Atomique et Ionique, Université Paris–Sud, 91405 Orsay Cedex, France

M. Cornille*
CNRS URA 176, Departement d'Astrophysique Relativiste et de Cosmologie, Observatoire de Paris, 92195 Meudon Cedex, France

K. Katsonis
Laboratoire de Physique des Gaz et des Plasmas, URA 073, Université Paris–Sud, 91405 Orsay Cedex, France
(Received 3 February 1994)

In the case of He-like ions, dielectronic recombination ends in the population of Li-like core excited states. Likewise the charge-exchange collision process involving *long-lived metastable* He-like ions ends in Li-like core excited states. The observation of satellites $1s2l2l' \rightarrow 1s^2 2l''$ and $1s^2 3l''$ leaves open a certain number of questions. The case of $O^{6+}(1s2s)^3S_1 + H_2$, $C^{4+}(1s2s)^3S_1 + H_2$, and $N^{5+}(1s2s)^3S_1 + H_2$ is considered. The satellites are seen, unpolluted by parent transitions on the one hand, and on the other hand the parent transitions are observed. But a further test of the capture process is significant: the ^4L to ^4L optical transitions in the vacuum ultraviolet range. The $n=4$ satellites in oxygen and nitrogen coincide with the $n=3$ parent transitions.

PACS number(s): 34.70.+e, 32.80.Dz

I. INTRODUCTION

The observations and theoretical investigations of spectra obtained by dielectronic recombination (DR) in a plasma allow diagnostics for electron temperature T_e and electron density N_e. In some cases, the models used are not sufficient to explain the evolution of the line intensity ratios Ix/Iw and Iz/Iw [1,2]. Then it is necessary to search for other collisional processes that can populate states similar to those obtained by DR and that stabilize in the same way, leading to an enhancement of the observed line intensities. The charge-exchange process (CX) is a good candidate. In general, this mechanism is taken into account under the following hypothesis: the ions are in the ground state and do not contribute to the formation of doubly excited ions. However, for He-like ions, the ^3L energy state nearest the ground state is the $1s2s\ ^3S_1$, and for low-Z atoms, it is a long-lived metastable state (τ is approximately some milliseconds for $Z \leq 10$).

In Sec. II, an overview on the collisions' main features is given; in Sec. III, the basic properties of Li-like core excited ions are reviewed and some cases of relevance to hot plasmas are considered. Finally, Sec. IV considers the incidence of CX, DR, and ionization rate coefficients on the problem of ionization equilibria of carbon, nitrogen, and oxygen, underlining that the consideration of CX of metastable ions is important.

*Author to whom correspondence should be addressed.

II. DR AND CX COLLISIONS' MAIN FEATURES

It is important to understand these collisions' main features, as cross section, population of excited states, and lifetimes, in order to determine afterwards the rate coefficients and the likelihood of the dominance of one process as opposed to the other, or of their cooperative effect.

A. Dielectronic recombination

For the process involving He-like ions in the ground state (where Z is the atomic number),

$$A^{(Z-2)+} + e^- \rightarrow A^{(Z-3)+**}, \tag{1}$$

it is understood that the electron energy is less than the excitation threshold. Moreover, it is known that along the He-like isoelectronic sequence, the DR cross section will vary as

$$\sigma \approx \frac{1}{Z^2} \tag{2}$$

and the populated doubly excited levels will be $1s2ln'l'$ with n' extending from 2 to ∞. As we show hereafter, these states, given that they all are above the first ionization limit in the Li-like sequence, will stabilize, sharing their decay among autoionization and radiation at each step of a cascade.

B. Charge-exchange processes

The change-exchange mechanisms have been observed in particular in highly charged ion sources. The simple

capture, which appears during the collision between a stripped ion and hydrogen atom, has been obtained theoretically [3–5]; this process is obtained now well understood. Theoretical investigation of ions with many open shells has not been done in general. However, many experimental efforts have been extensively developed, which allow one to measure cross sections for different ionization stages and different atomic partners of the collision. In particular, it is possible to establish experimental scaling laws for the cross sections [6,7]. The predicted values present an uncertainty of ±15%. In general, for charge-exchange collisions at low velocities ($V<1$ a.u.),

$$A^{q+}+B\rightarrow A^{(q-1)+}+B^{+}\ , \tag{3}$$

the cross section is almost constant and given by the formula

$$\sigma_{q,q-1}\simeq(4.00\pm0.7)\times10^{-12}\frac{q}{[I_0\ (\mathrm{eV})]^3}\ \mathrm{cm}^2\ , \tag{4}$$

where q is the charge of the incoming ion and I_0 (eV) is the ionization potential of the target. Furthermore, during the collision the electron capture leads to a state-selective populating of the projectile: one or two levels with specific principal quantum numbers n. Different Landau-Zener models allow one to predict the principal quantum number of the most populated levels [8]. If we consider a quasihydrogenic behavior of the system during the electron transfer from the atom to the ion, it has been shown that the most populated capture level corresponds to a quantum number n of the order $n\approx q^{3/4}/[I\ (\mathrm{a.u.})]^{1/2}$ [9] (where I is the ionization potential of the atom in atomic units).

In general, the distribution of the population of each l in the level n is not predicted theoretically, but experimentally it has been possible to show that the collision velocity is the leading element of the distribution in these sublevels. This reflects the evolution of radial and angular couplings as a function of the velocity of the incoming ion. Indeed, in all experiments where the total cross sections σ are constant the partial cross sections σ_l evolve with the velocity of the colliding ion. Moreover, the charge-exchange cross sections are very large (of the order of 10^{-15} cm^2 and sometimes even larger). This leads to a large associated collision rate coefficient $\langle\sigma_{\mathrm{CX}}V\rangle$, of the order of 10^{-7}–10^{-8} cm^{3}s^{-1}. These cross sections and rate coefficients depend on the charge q of the ion and are not much influenced by the electronic configuration of the ion for an ion charge q.

III. CX INVOLVING THE FORMATION OF Li-LIKE CORE EXCITED IONS

We will first consider and review the general properties of Li-like core excited ions. Although they have in general the features of states populated in DR, it is of interest to understand their structure and properties in some detail.

A. Core excited Li-like ions

Attention was focused on the Li-like core excited ions for which the electronic structure is well known. The position of the energy levels E_n with respect to the ground level and to the first ionization limit of $1s^2\,{}^1S_0$ allow one to predict that all the levels stabilize via spontaneous emission (cascades) and/or autoionization [7]. In general the autoionization takes place towards the nearest continuum $1s^2\,{}^1S_0$. The single capture that occurs during the collision of O^{6+}, C^{4+}, and N^{5+} with H_2 has been studied theoretically and experimentally by many authors. In the present work, we consider the single capture by long-lived metastable He-like ions $(1s2s)^3S_1$; in particular, the single capture that occurs during the collision of $O^{6+}(1s2s)^3S_1$ with H_2 at a velocity of $0.39V_0$ with V_0 the atomic unit of velocity). In order to analyze the data for $O^{6+}(1s2s)^3S_1$, the energy levels, transition probabilities, and Auger rates have been calculated for $(1s2lnl')^{2,4}L_J$ with $n=2,3$ by Bliman *et al.* [10] and $n=4$ by Suraud *et al.* [11]. The Li-core excited energy levels with corresponding total fluorescence yields are given in Fig. 1 for the case of O^{5+}. The total fluorescence yield for each level is defined as

$$\omega_T=\frac{\sum A_{ij}}{\sum A_{ij}+\sum A_a}\ , \tag{5}$$

where A_{ij} and A_a are, respectively, the radiative transition probabilities and the autoionization rates. The line fluorescence yield is obtained by multiplying the total fluorescence yield by the branching ratio of the specific transition. It is important to emphasize that, for Li-like ions, it is possible to observe experimentally two types of multiplets: ^2L and ^4L. But when dealing with ^2L states it is necessary to carefully differentiate between the singlet core $1s2l\,{}^1L$ and the triplet one $1s2l\,{}^3L$, which end in energetically different states. Moreover, these lithiumlike states do stabilize differently. The sharing between fluorescence and autoionization is different. All quartet states ^4L are generally metastable against autoionization and their decay is radiative. However, the lowest-lying quartet states $1s2s2p\,{}^4P^o_J$ and $1s2p^2\,{}^4P_J$ deserve very careful attention. Depending upon the value of J, the fluorescence yield will vary significantly: $1s2s2p\,{}^4P^o_{1/2,3/2}$ have an increasing fluorescence yield (see Fig. 2), whereas $1s2s2p\,{}^4P^o_{5/2}$ autoionizes to $1s^2\,{}^1S_0$ by spin-spin interaction, at low Z values. The same remarks are nearly valid for $1s2p^2\,{}^4P_{1/2,3/2}$ (Fig. 3). For doublet states ^2L, as is shown in Fig. 1, the levels with singlet core ^1L generally lie above those with the triplet core ^3L. This situation is reproduced along the isoelectronic sequence; Figs. 4(a)–4(c) show the fluorescence yield of $1s2s3l$ versus atomic number $Z\leq10$. As we discuss below, in some specific cases the charge-exchange collision process ends in populating a very narrow set of excited levels: in the limit of low-energy collisions ($E\leq25$ keV amu) the most probably populated level is nearly equal to

$$n\approx\frac{q^{3/4}}{[I(\mathrm{a.u.})]^{1/2}}\ , \tag{6}$$

where q is the incident ion charge, I is the ionization potential of the atom in atomic units, and n is the principal quantum number of the most populated level. The sharing among sublevels is not statistical and depends upon

the collision velocity. However, the sharing among ^2L and ^4L is globally statistical. The stabilization at each step in the cascade is shared between a photon emission and autoionization, as shown in Fig. 5.

B. Some CX cases of relevance to hot plasmas involving H_2

It is well known that hydrogen plasmas are contaminated by impurities such as carbon, nitrogen, and oxygen. For these elements, the He-like metastable ion $1s2s\ ^3S_1$ state is long lived; the lifetime is $\tau \geq 10^{-4}$ s. Their radiative decay is associated with a magnetic-dipole transition M_1 nearly forbidden for low-Z atoms.

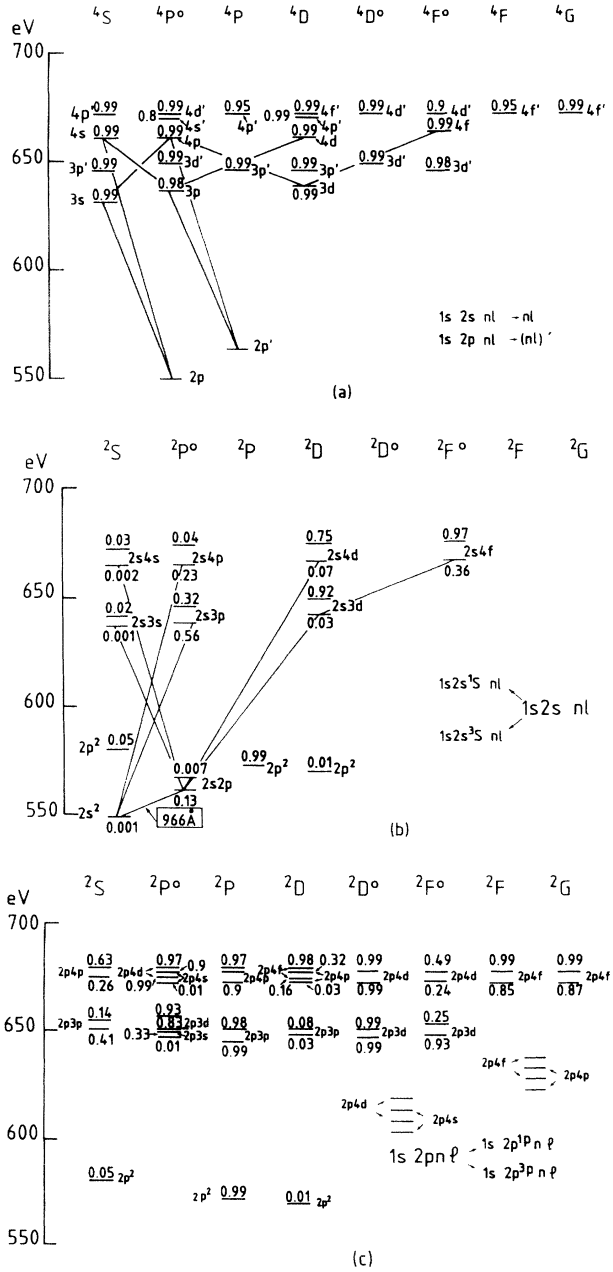

FIG. 1. Li-core excited oxygen energy levels with corresponding fluorescence yields. Energies in eV are given above ground state $1s^22s\ ^2S_{1/2}$. (a) Quartet states $1s2s2p \rightarrow 1s2snl$ and $1s2p^2 \rightarrow 1s2p(nl)$. (b) Doublet states $1s2snl$. For each nl the lowest-lying level is $1s2s\ ^3Snl$ whereas $1s2s\ ^1Snl$ is slightly higher. (c) Doublet states $1s2pn'l'$. Each $n'l'$ has two values: the lowest one is $1s2p\ ^3Pn'l'$; the highest one is $1s2p\ ^1Pn'l'$.

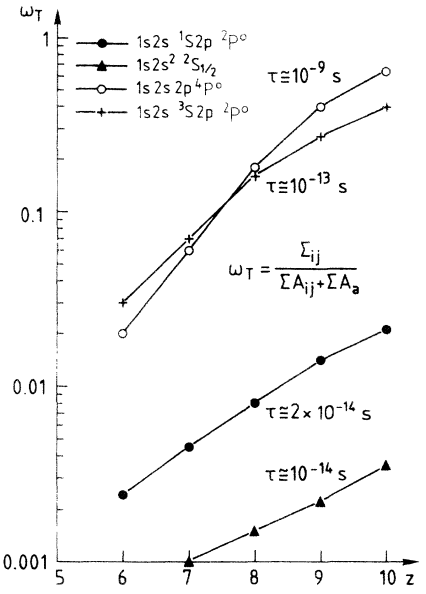

FIG. 2. Li-like ions fluorescence yields ω_T of $1s2s\ ^1S2p\ ^2P^o$, $1s2s^2\ ^2S$, $1s2s2p\ ^4P^0$, $1s2s\ ^3S2p\ ^2P^o$ versus atomic number Z.

1. Experimental procedure

A charge and mass-analyzed He-like ion beam at $10q$ keV is passed through a differentially pumped collison cell (inner pressure $=3.5\times10^{-5}$ Torr of H_2). A Bragg diffractometer (equipped with a flat crystal with $2d$ ap-

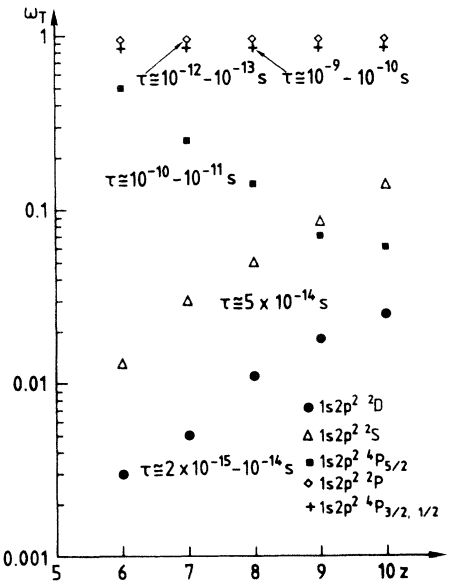

FIG. 3. Li-like ions fluorescence yields ω_T of $1s2p^2\ ^2D$, ^2P, ^2S, and $1s2p^2\ ^4P_{3/2,1/2}$ and $1s2p^2\ ^4P_{5/2}$ versus atomic number Z.

propriate to the wavelength interval and used in conjunction with a low-pressure flowing gas proportional counter) looking at 90° to the beam direction directly into the collision chamber records the soft-x-ray emissions [12]. The vacuum ultraviolet (vuv) emission in the wavelength range 100–200 Å is recorded, making use of a Rowland circle mount spectrometer equipped with a 3-m grating with 300 lines /mm. A detector based on multichannel plates and the resistive anode readout technique is used [13]. The beam gas interaction length viewed by both spectrometers is approximately 2 cm. Under those conditions, radiative emissions following single-electron capture are obtained. An electron spectrometer records the Auger electron emitted at an angle of 10° from the incident ion direction [5].

2. *Oxygen ion O^{6+}*

To illustrate the experimental situation, Figs. 6(a) and 6(b) show, respectively, in the case of oxygen the K

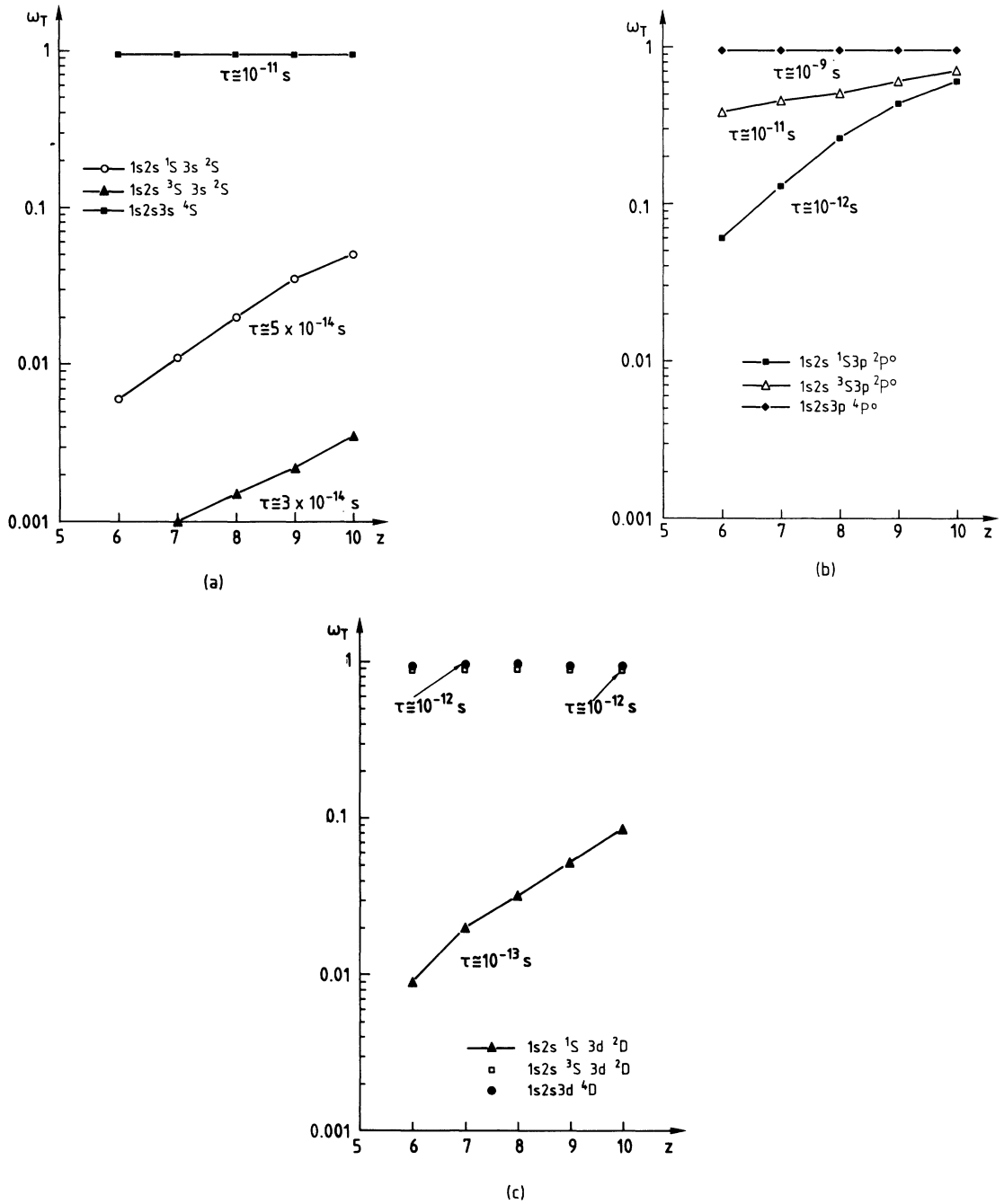

FIG. 4. Fluorescence yield ω_T along the isoelectronic sequence. (a) Fluorescence yields of $1s2s\,^1S\ 3s\,^2S$, $1s2s\,^3S3s\,^2S$, and $1s2s3s\,^4S$; (b) fluorescence yields of $1s2s\,^1S3p\,^2P^o$, $1s2s\,^3S3p\,^2P^o$, and $1s2s3p\,^4P^o$; (c) fluorescence yields of $1s2s\,^1S3d\,^2D$, $1s2s\,^3S3d\,^2D$, and $1s2s3d\,^4D$.

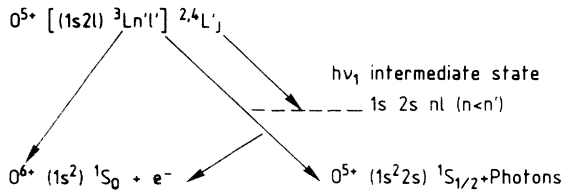

FIG. 5. The stabilization of the Li-like ion O^{5+}.

fluorescence recorded in the collision

$$O^{7+}+H_2 \rightarrow O^{6+}(1snl)^{1,3}L_J+H_2^+ \quad . \tag{7}$$

The decays $1snp \rightarrow 1s^2\,{}^1S_0$ are seen: The He-like parent transitions are seen in Fig. 6(a), while Fig. 6(b) recorded at the same velocity shows the transitions due to the K fluorescence of Li-like core excited oxygen ions following the capture collision:

$$O^{6+}(1s2s)^3S_1+H_2 \rightarrow O^{5+}(1s2ln'l')^{2,4}L_J+H_2^+ \quad . \tag{8}$$

In this case, the capture level n is typically $n=4$ and the different radiative transitions are unambiguously identified. Moreover, comparing the satellite positions and the parent transitions, it is seen that $1s2s4p$ is coincident with the He-like transition $1s3p \rightarrow 1s^2$. The autoionization spectrum shows that the continuum to which the Li-like core excited states $1s2ln'l'$ decay is the He-like ground state $1s^2\,{}^1S_0$. The low-energy peaks are due to cascade feed from the capture level. In Fig. 7 the highest energy peak corresponds to the capture level and the lowest are due to cascade population. The most intense peaks in the low-energy part of the spectrum are associated with the autoionization of $1s2s2p\,{}^4P_{5/2}$ and $1s2p^2\,{}^4P_{5/2}$ [3].

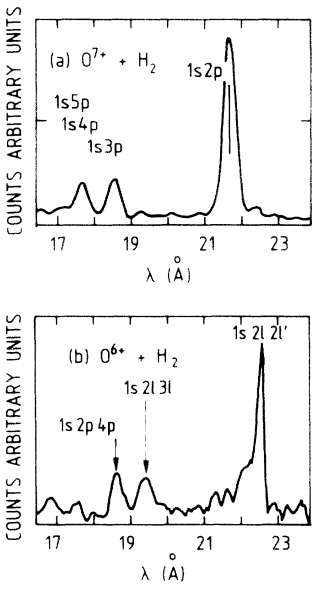

FIG. 6. (a) X-ray spectrum emitted in the single-electron capture collision $O^{7+}+H \rightarrow O^{6+}(1snl)^{1,3}L+H^+$. The K transitions correspond to $O^{6+}(1snp)^{1,3}L \rightarrow O^{6+}(1s^2)^1S+h\nu$. (b) X-ray spectrum emitted in the single-electron capture collision $O^{6+}(1s2s)^3S+H \rightarrow O^{5+}(1s2ln'l')^{2,4}L+H$. The K fluorescence of core excited Li-like oxygen corresponds to $O^{5+}(1s2ln'l')^{2,4}L \rightarrow O^{5+}(1s^22l)^2L+h\nu$.

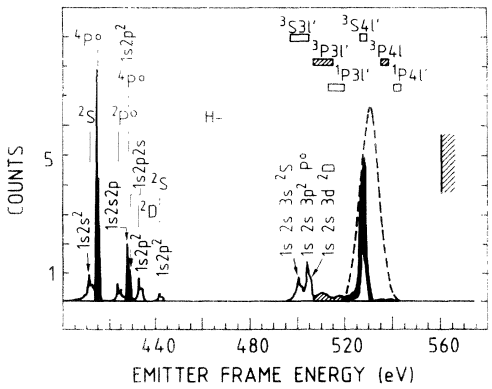

FIG. 7. Autoionization spectrum following the capture collision involving metastable He-like oxygen ion O^{6+}.

3. *Carbon ion* C^{4+}

In this case, the charge-exchange collision with H_2 populates mostly $n=3$. The photon x-ray spectrum shows a set of lines $1s2l3p$ decaying directly to $1s^22l$. This is well understood considering the fluorescence yield w_T of $1s2s2p\,{}^4L_J$, which is equal to 0.003 [14]. This means that nearly all $1s2l2l'$ (particularly, $1s2s2p\,{}^2P_J^o$ and $^4P_J^o$) nearly 100% autoionize and are not expected to be present in the photon spectrum. In Fig. 8 are shown the K photon spectra emitted by $C^{4+}(1snp \rightarrow 1s^2)$ obtained in the CX collision $C^{5+}+H_2$ [Fig. 8(a)], while Fig. 8(b) shows the x-ray spectrum from $C^{4+}(1s2s)^3S_1+H_2 \rightarrow C^{3+}(1s2l3l)^{2,4}L_J+H^+$.

The Auger spectrum obtained by Mack [3] shows an intense group of lines of energies of 220–240 eV (stabilization of $1s2l2l'\,{}^{2,4}L_J$ populated by cascades) and a group of lines of energies around 270 eV emitted from the levels directly populated ($n=3$).

4. *Nitrogen ion* N^{5+}

As nitrogen is intermediate between oxygen and carbon, the capture level mostly populated is $n=3$. with a small fraction going to $n=4$. To determine the position of the transitions $1s2ln'l' \rightarrow 1s^22l$, $1s^2n'l'$, the He-like spectrum is recorded. Figure 9(a) shows the He-like spectrum and Fig. 9(b) recorded in the same wavelength interval shows unambiguously the decay of the Li-like core excited levels.

The complementary part of the photon stabilization Auger spectrum was already observed: Mack [3] shows two groups of peaks, the capture levels' direction population giving peaks of energies between 360 and 400 eV, while peaks corresponding to a cascade feed of $1s2l2l'$ are seen in the energy interval 320–340 eV.

The difference observed in the behavior of $1s2l2l'$ for the three ions is basically related to the fluorescence yields of the levels (see O^{6+},C^{4+},N^{5+}, in Figs. 2 and 3). The described experiments show that the He-like spec-

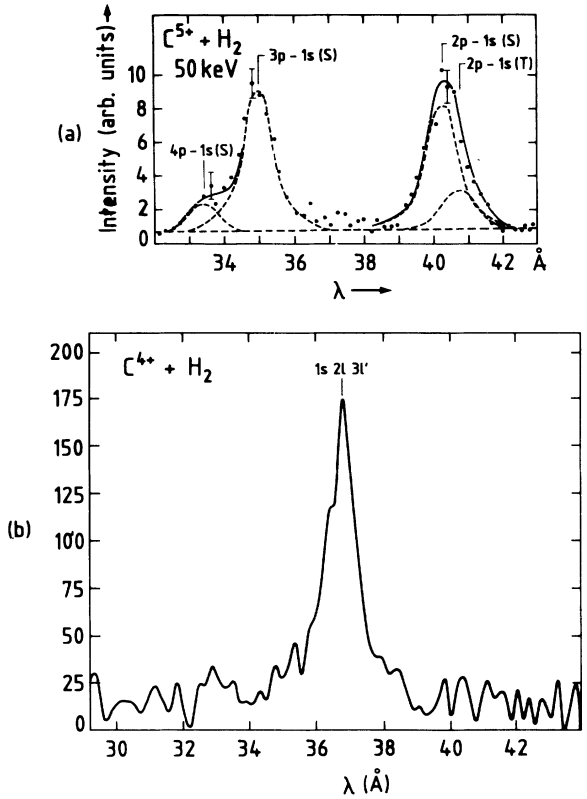

FIG. 8. (a) Photon spectrum for the emissions following the CX process $C^{5+}(1s)^2S_{1/2}+H_2 \rightarrow C^{4+}(1snl)^{1,3}L + H_2^+$. (b) Photon spectrum from $C^{4+}(1s2s)^3S_1+H_2 \rightarrow C^{3+}(1s2ln'l')^{2,4}L+H_2^+$.

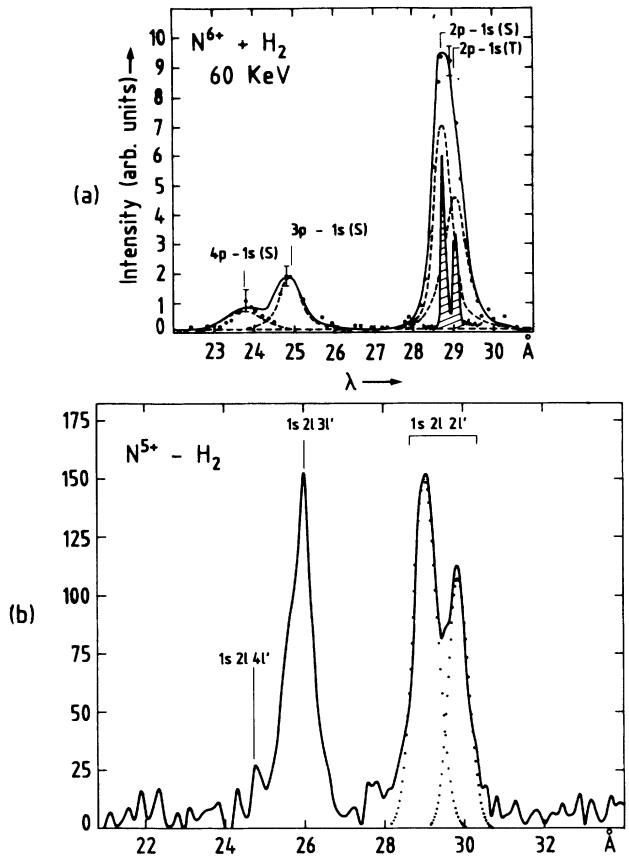

FIG. 9. (a) Emissions following the CX process $N^{6+}+H_2 \rightarrow N^{5+}(1snl)^{1,3}L+H_2^+$. (b) Photon spectrum from $N^{5+}(1s2s)^3S_1+H_2 \rightarrow N^{4+}(1s2ln'l')^{2,4}L+H_2^+$.

trum is unpolluted by satellites on the one hand, whereas on the other hand the satellites are alone (no parent transitions).

IV. RATE COEFFICIENTS AND THE IONIZATION EQUILIBRIUM

The fact that DR and CX involving metastable ions end in populating Li-like core excited states, raises two important questions: what are the rate coefficients for these processes and what is the consequence on the ionization equilibrium?

A. CX rate coefficients

Low-energy (down to 10 eV/amu) charge-transfer calculations for $H+C^{q+} \rightarrow C^{(q-1)+}+H^+$ ($q=1-6$) by Katsonis and Maynard [14] have shown that these collisions are essentially Coulomb-like: The cross sections can be estimated with the charge-transfer Monte Carlo (CTMC) method using a Coulomb potential in a large energy range. Consequently, this method has been used to calculate the charge-transfer cross sections of C^{4+} and O^{6+} colliding with H. The corresponding rate coefficients have been calculated after integrating over a Maxwellian distribution for a hydrogen plasma of temperature T_{keV}. The results are given in Fig. 10; the rate coefficients A presented in this figure are also given in parametric form in 10^{-8} cm^{3}s^{-1}, using the representation

$$A/n = y(a+by^c)/(1+dy^c+fy^g) ,$$

where n is the density in cm^3 and y is the energy in keV. The corresponding values of the parameters are

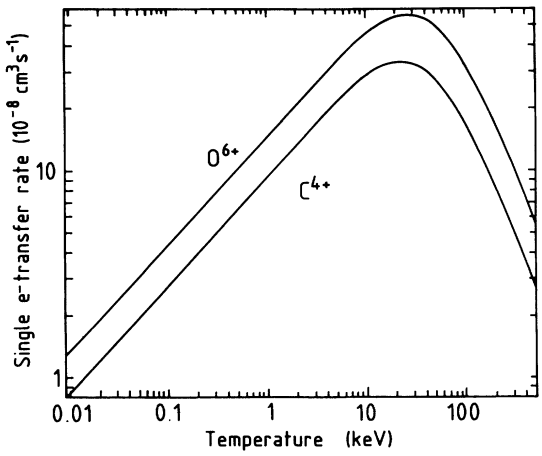

FIG. 10. Single charge-transfer rate coefficients A versus temperatures in keV for collision of carbon and oxygen ions ($q=4$ and 6) with hydrogen.

$a=8.3$, $b=0.94$, $c=1.0$, $d=0.0116$,

$e=2.57$, $f=1.30\times10^{-4}$, $g=4.6$ for C^{4+}

$a=13.3$, $b=1.20$, $c=1.0$, $d=0.0105$,

$e=2.50$, $f=0.86\times10^{-4}$, $g=4.6$ for O^{6+}.

Note that if one wants to consider the carbon ions as having also a Maxwellian distribution, the combined result is easily calculated using a modified temperature $T_{\text{mod}}=(T_i+M_iT_H)/M_i$, where T_H and T_i are the temperatures of the H and of the C and O ions and $M_i=12$ and 16.

B. DR rate coefficients

In order to appreciate the influence of the various competing atomic processes in plasmas including multicharged ions, the charge-transfer rate coefficients of Fig. 10 are to be compared with the rate coefficients of dielectronic recombination for the same ions (C^{4+},O^{6+}). In the case of highly ionized He-like ions, dielectronic recombination rate coefficients have been calculated by Younger [15] and Nilsen [16], both for astrophysical (solar corona) and laboratory (magnetic fusion) plasmas. A distorted-wave method has been used by Younger [15] mainly in the *LS* coupling scheme to calculate the rates for several He-like ions. Nilsen [16] used relativistic configuration wave functions for evaluating the total dielectronic recombination rates for multiply charged ions with $10\leq Z\leq 54$. These calculations constitute an improvement over the older Burgess [17] and Merts-Cowan-Magee [18] formulas. Here, the dielectronic recombination rate coefficients for the He-like ions C^{4+} and O^{6+} have been evaluated on the basis of the work of Younger [15] and of Nilsen [16]. In Fig. 11 these rates are given for an extended energy region. In comparison with Fig. 10 it is easy to realize that, even for the most favorable energy values, the effect of the dielectronic recombination is orders of magnitude less than the effect of the charge transfer.

The CX rate coefficient can be compared with the DR rate coefficient. For example, Andersen *et al.* [19] have measured DR rate coefficient for $O^{6+}(1s2s)^{3,1}S$. The obtained values are of the order of 10^{-10} cm^3 s^{-1}; the CX rates are larger than DR ones and this allows an understanding of the dynamical behavior of Li-like core excited ions.

C. Ionization rate coefficients

We also compare the aforementioned rates with the electron collision ionization rates for the same ions (C^{4+},O^{6+}), a competing process, and also for the corresponding Li-like ions ionization, an inverse process populating the He-like levels. The rates presented in Fig. 12 are taken from the well known evaluation from Bell *et al.* [20] and Kato, Masai, and Arnaud [21]. Such a comparison was previously presented by Younger [15], but due to a number of misprints occurring in the paper the appreciation was not clear. Although smaller than the charge-transfer ones, these rates are bigger than the dielectronic recombination ones for low-Z ions; nevertheless, for high-Z ions, even if the dielectric recombination rates are smaller, the electron collision ionization rates are increasing only for higher energies, and consequently the dielectronic recombination is more important for low-energy regions.

The ionization rates are calculated for the ground-state ions. It is clear that a calculation for the metastable ions would give ionization rates intermediate between the values for the Li-like and He-like ground-state ions.

D. Ionization equilibrium

Even though the number density of metastables is small (in current experiments involving beams extracted from electron-cyclotron-resonance ion sources—a hot plasma device—we have always measured total He-like ion beam metastable fractions of the order of 10% of the total He-like ion beam), the rate coefficient times the He-like ion number density is still in favor of the CX for populating the Li-like core excited levels. The simplest ionization equilibrium model (Coronal model) is probably

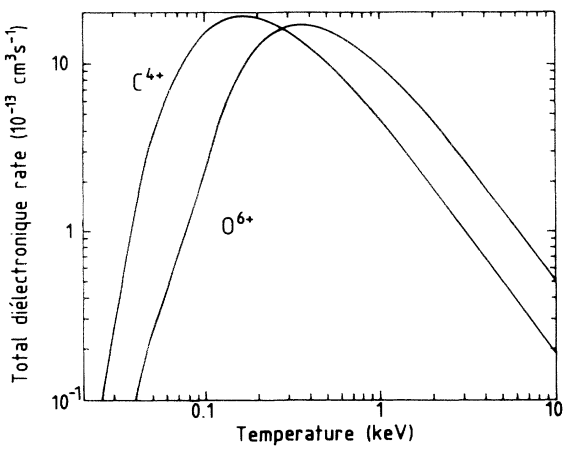

FIG. 11. Total dielectronic rate versus temperature in keV of carbon and oxygen ions ($q=4$ and 6).

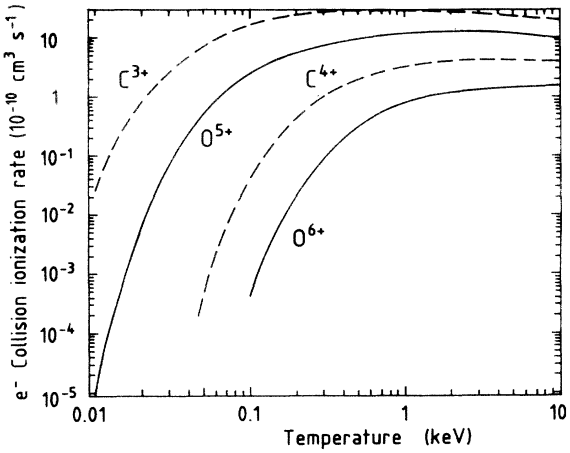

FIG. 12. Collision ionization rate versus temperatures in keV of carbon ions ($q=3$ and 4) and oxygen ions ($q=5$ and 6).

not sufficient to describe the behavior of the He-like ions. For the He-like ionization stage, the simplest model should include the following terms in the common rate equations:

$$\frac{dn_{(Z-2)^+}}{dt} = n_e n_{(Z-3)^+} \langle \sigma V_e \rangle_{\text{ioniz}} - n_e n_{(Z-2)^+} \langle \sigma V_e \rangle_{\text{DR}} - n_0 n^*_{(Z-2)^+} \langle \sigma v \rangle_{\text{CX}} - n_e n^*_{(Z-2)^+} \langle \sigma V_e \rangle_{\text{ioniz}} ,$$

where $(Z-2)^+$ is the charge of He-like cores and V_e and v are the electron and ion velocities, respectively, and n^* is the metastable number density. In typical times of order 10^{-12} s, the fraction that autoionizes restores the ground-state He-like ion $1s^2\,{}^1S_0$.

V. CONCLUSION

We have shown that the charge-exchange collisons facilitate the distinction of levels likely to be identified. It is important to stress that there are many other situations where charge exchange and dielectronic recombination cooperate for emission of satellites. Therefore Be-like ions, having above their ground state a long-lived metastable state $1s^2 2s2p\,{}^3P_0$, and Ne-like ions, where the $2P^5 3s\,{}^3P_0^o$ metastable state cannot decay to the respective ground state, have to be carefully investigated. Account must be taken of the stabilization of the Li-like core excited ions: they share their decay through photon radiation and autoionization, the last mechanism restoring ground-state He-like ions.

[1] M. Bitter, K. W. Hiell, M. Zarnstorff, S. von Goeler, R. Hulse, L. C. Johnson, N. R. Sauthoff, S. Sesnic, K. M. Young, M. Tavernier, F. Bely-Dubau, P. Faucher, M. Cornille, and J. Dubau, Phys. Rev. A **32**, 3011 (1985).

[2] M. Bitter, M. Hsuan, V. Decaux, B. Grek, K. W. Hill, R. Hulse, L. A. Kruegel, D. Johnson, S. von Goeler, and M. Zarmstorff, Phys. Rev. A **44**, 1796 (1991).

[3] E. M. Mack, Ph.D. thesis, Rijks Universiteit Utrecht, The Netherlands, 1987.

[4] S. Bliman, D. Hitz, B. Jacquot, C. Harel, and A. Salin, J. Phys. B **16**, 2849 (1983).

[5] M. Boudjema, PhD. thesis, Université d'Alger, 1990.

[6] A. Müller and E. Salzborn, Phys. Lett. **62A**, 391 (1977).

[7] S. Bliman, A. Bonnefoy, J. J. Bonnet, S. Dousson, A. Fleury, D. Hitz, and B. Jacquot, Phys. Scr. **63**, (1983).

[8] H. Ryufuku, K. Sasaki, and T. Watanabe, Phys. Rev. A **21**, 745 (1980).

[9] R. Mann, F. Folkmann, and H. F. Meyer, J. Phys. B **14**, 1161 (1981).

[10] S. Bliman *et al.*, J. Phys. **25**, 2065 (1992).

[11] M. G. Suraud, S. Bliman, D. Hitz, J. E. Rubensen, J. Nordgren, J. J. Bonnet, M. Bonnefoy, M. Chassevent, A. Fleury, M. Cornille, E. J. Knystautas, and A. Barany, J. Phys. B **25**, 2363 (1992).

[12] A. Fleury, J. De Bernardini, M. Bonnefoy, S. Bliman, J. J. Bonnet, and M. Chassevent, Nucl. Instrum. Methods Phys. Res. Sect. B **14**, 353 (1986).

[13] J. Nordgren and R. Nyholm, Nucl. Instrum. Methods Phys. Res. Sect. A **246**, 314 (1986).

[14] K. Katsonis and G. Maynard, in *Proceedings of the IAEA Technical Committee Meeting on Fusion Reactor Technology,* edited by H. W. Drawin and R. Janev (UNIPUB, Lanham, MD, 1992), p. 29.

[15] S. M. Younger, J. Quant. Spectrosc. Radiat. Transfer **29**, 67 (1983).

[16] J. Nilsen, J. Phys. B **19**, 2401 (1986).

[17] A. Burgess, Astrophys. J. **141** 1588 (1965).

[18] A. L. Merts, R. D. Cowan, and N. H. Magee, Jr., Los Alamos National Laboratory Report No. LA-6220-MS, 1976 (unpublished).

[19] L. H. Andersen, P. Hvelplund, H. Knudsen, and P. Kvistgaard, Phys. Rev. Lett. **62**, 2656 (1989).

[20] K. L. Bell, H. B. Gilbody, J. G. Huges, A. E. Kingston, and F. J. Smith, J. Phys. Chem. Ref. Data **12**, 891 (1983).

[21] T. Kato, K. Masai, and M. Arnaud, Report No. NIFS-DATA-14, 1991 (unpublished).